A new intermolecular potential for hydrazine clusters: Structures and spectra

T. A. Beu,[a] U. Buck, and J. G. Siebers
Max–Planck–Institut für Strömungsforschung, Bunsenstraβe 10, D-37073 Göttingen, Germany

R. J. Wheatley[b]
Department of Chemistry, University of Durham, Durham, DH1 3LE, England

(Received 25 June 1996; accepted 24 September 1996)

The structures of small hydrazine clusters from the dimer to the hexamer have been calculated using a standard site-site intermolecular potential and a newly developed systematic approach which is essentially based on monomer properties. Aside from the repulsive and the attractive dispersion and induction interaction special care is taken for the determination of the electrostatic interaction which is represented by a distributed multipole expansion and a penetration correction. Based on these potentials the vibrational spectra of the N-N stretching and the asymmetric NH_2 wagging mode are calculated using degenerate perturbation theory. While the small shifts of the N-N stretching mode are fairly well reproduced by both potential models, large differences are predicted for the asymmetric NH_2 wagging mode. Here, redshifts of -30 cm^{-1} are calculated for the standard and blueshifts of 100 cm^{-1} are obtained for the systematic potential in agreement with experiment. The analysis shows that the reason for this behavior is the careful treatment of the electrostatic term in this model. © *1997 American Institute of Physics.* [S0021-9606(97)01501-8]

I. INTRODUCTION

Clusters of stable molecules are usually bound by weak van der Waals forces or hydrogen bonds. They often exhibit different structures than their two limiting cases, the dimer and the solid crystal.[1,2] Structural information is best obtained from high resolution spectroscopy using absorption[3,4] or opto-thermal detection[5,6] methods. The spectroscopy is, however, restricted to small clusters. In order to obtain information on larger clusters, special techniques for the selection of single cluster sizes have to be applied. Unfortunately, the simple mass spectrometric detection does not work, since strong fragmentation during the ionization process destroys the correlation between the measured ionic cluster and its neutral precursor.[1,7] To overcome this problem, we have used the momentum transfer in a scattering experiment with atoms to prepare a cluster of one size.[1,7,8] In combination with infrared photodissociation spectroscopy this is a powerful tool to get information as a function of the cluster size.[2] Typically, in such predissociation experiments a beam of clusters containing ir-active molecules is formed in a supersonic nozzle and expanded into a vacuum chamber, where an intramolecular mode of vibration is excited by ir-radiation. Energy relaxation may subsequently lead to predissociation of the clusters, causing a decrease in the beam signal.[5] As a direct result of the mutual interaction of the molecules within the cluster, the spectral bands found in these experiments appear shifted (and sometimes also split) with respect to the corresponding gas phase absorption frequencies. For van der Waals systems the frequency shifts are typically of several wave numbers, while for the X-H vibrations of hydrogen bonded systems the shifts can amount to hundreds of cm^{-1}.

The comparison of the measured data with calculations of the ir-spectra of these clusters gives detailed information on their structure. Recently, we have developed a perturbation approach for the evaluation of the frequency shifts of homogeneous molecular clusters[10] with a generalized result for degenerate states.[11] The basic idea is to treat the anharmonic intramolecular force field and the intermolecular potential as a quantum mechanical perturbation of the molecular vibrations, described in the normal mode approach. It is referred to as *frozen molecule approach* (FMA) in the further course of this work.

The most detailed results up to now have been obtained for methanol clusters for which the measured CO stretch[13–15] and the OH stretch[16,17] modes have been analyzed and interpreted in terms of detailed structural information.[9,10] Similar results have been obtained for small SF_6 clusters.[12] Hydrazine clusters are another interesting system for which the antisymmetric NH_2 wagging mode ($\nu_{12}=937$ cm^{-1}), and the symmetric N-N stretching mode ($\nu_5=1098$ cm^{-1}) have been measured from the dimer to the hexamer.[18] The former mode exhibits large blueshifts up to more than 100 cm^{-1}, while the latter one shows almost size-independent small shifts.

In the present paper we apply the FMA formalism to the investigation of the spectral line shifts of hydrazine clusters from dimer to hexamer. For that purpose the intramolecular force field of Ref. 19 is used in combination with two intermolecular potentials. The first one is the EPEN/2 model of Snir et al.[20] which consists of charges, repulsive and attractive centers placed at the positions of the atoms, the lone pair electrons, and on the bonds. The second one is systematically calculated from properties of the monomers and contains the

[a]Permanent address: University ''Babeş-Bolyai,'' Department of Theoretical Physics, 3400 Cluj-Napoca, Romania.
[b]Present address: Department of Chemistry, University of Nottingham, Nottingham NG7 2RD, England.

electrostatic interaction using a distributed multipole expansion and a penetration component, the repulsion, and the attractive induction and dispersion terms.[21]

The calculated structures for the two potentials differ in details but show the same general trends, chain structures for the dimers, cyclic structures for the trimers and three dimensional behavior for the larger clusters. The comparison of the calculated lineshifts, however, with the published experimental data exhibits appreciable differences for the two potentials. Only the predictions for the NH_2 wagging mode based on the systematic potential model are in good agreement with the measurements. Since the experimental data are partly incomplete, we have carried out new measurements and a detailed comparison with these new data is published in the paper following this one.

The paper starts with a description of the two potential models. Then the resulting structures for the different cluster sizes are discussed. Based on these results the frequency shifts are calculated using the frozen molecule approach. Finally, the results for the two potentials are compared and the general behavior with respect to the different potential terms is discussed for the systematic model.

II. INTERMOLECULAR POTENTIAL MODELS

A. The EPEN/2 potential

One of the most critical aspects of matching structure and frequency shift calculations for clusters of molecules with experimental data is the choice of a realistic intermolecular potential function. Due to the complexity of such calculations, two somewhat contradictory prerequisites for the potentials are usually imposed: accurate description of the experimental evidence, and a relative simplicity of the evaluation. In many cases, site-site potentials seem to be competitive candidates for tractable numerical solutions. The molecular interactions are modelled through distributed interaction *sites*, which account for the nuclei and electronic charge clouds, and whose relative positions remain unchanged within the molecules. Such an approach allows for the total interaction energy of the molecular cluster being expressed solely from the pairwise molecular interactions. Three-body and higher order terms are not considered explicitly. However, evaluating derivatives of the interaction energy with respect to vibrational coordinates of a particular molecule, implies displacing the atomic sites along the normal modes of vibration.

Among the potential energy hypersurfaces available in the literature for the description of the molecular interactions within the hydrazine clusters, we have chosen the model called EPEN/2 (potential based on the interaction of electrons and nuclei) by Snir, Nemenoff and Scheraga.[20] In this model, positive charges are located at the atomic nuclei, which carry a charge of $Z-2$, where Z is the atomic number, excepting hydrogen which carries a charge of $+1$. Negative charge centers are located off the nuclei, and their charges are equal to -1 or -2, corresponding to single electrons, or electron pairs, respectively. The bonding electrons are located along the bonds, while the lone-pair (or π) electrons are located off the bonds. However, the negative charge centers should be regarded strictly as centers of interaction, which do not represent the actual electron distribution. Thus the term ''electrons'' is used just for convenience. Molecules are assembled from fragments. The distances between the charge locations and the heavy atoms are fixed in the fragments and are determined by fitting to experimental data (spectroscopic studies on single molecules in the gas phase, crystallographic studies, thermodynamic properties of crystals and liquids).

TABLE I. EPEN/2 parameter values for hydrazine.

Parameter	Value
Distance of N-H electrons from N nucleus	0.64600 Å
Distance of N-N electrons from N nucleus	0.48239 Å
Distance of lone-pair electrons from N nucleus	0.28200 Å
A_{ii} (saturated N electron)	27567.22 kJ/mol
B_{ii} (saturated N electron)	4.03459 $Å^{-1}$
C_{ii} (saturated N electron)	149.09 kJ/mol $Å^6$

The functional expression of the EPEN/2 potential has the form

$$U_{ab}=\frac{1}{4\pi\epsilon_0}\sum_{i,j}\frac{q_iq_j}{r_{ij}}+\sum_{k,l}g_kg_l\left(A_{kl}e^{-B_{kl}r_{kl}}-\frac{C_{kl}}{r_{kl}^6}\right). \quad (1)$$

The first sum describes the electrostatic interaction between site i of molecule a and site j of molecule b and runs over all atomic and bond sites with lone pair electrons included. The hydrazine molecule is built up from two amino groups, for which we have, aside from the N atom ($q=5$) and the two H atoms ($q=1$), the two N-H bonds ($q=-2$), the one bond lying along the N-N direction ($q=-1$), and the two N lone-pair electrons ($q=-2$), constrained to lie along the sum of the unit vectors of the three bonds formed with the nitrogen. For all bond sites of the amino group distances from the nitrogen atom are fixed parameters. With the charges q_i and q_j in units of the elementary charge, the distance r_{ij} between the charges in Ångstrom, and the constant factor of 1389.35 the energy is given in kJ/mol.

The second sum describes the nonbonded interaction between site k of molecule a and site l of molecule b and runs over the bond sites with the lone pair electrons included. Each type of bond is assigned a set of parameters A_{kk}, B_{kk}, and C_{kk}, the model coefficients A_{kl}, B_{kl}, and C_{kl} resulting from standard combination rules

$$A_{kl}=\sqrt{A_{kk}A_{ll}},\quad B_{kl}=(B_{kk}+B_{ll})/2,\quad C_{kl}=\sqrt{C_{kk}C_{ll}}. \quad (2)$$

The dimensionless weights g_k, g_l are 2 for all sites except for the N-N bond for which 1 is used. The positions of the sites and the A_{kk}, B_{kk}, and C_{kk} parameters for hydrazine are given in Table I. The monomer configuration is taken from Ref. 22 and the electron sites are built in according to the EPEN/2 specifications. The values of the relevant geometrical parameters are listed in Table II.

A rather delicate numerical aspect when calculating potential derivatives regards the handling of bond sites, since

TABLE II. Geometry of hydrazine.

Parameter	Value
N-H bond length	1.016 Å
N-N bond length	1.446 Å
HNH angle	106.00°
NNH angle	108.85°
θ_{tor} - dihedral angle between amino groups	88.05°

TABLE III. Atomic coordinates for hydrazine, expressed in the molecular axis system described in the text. All coordinates are in Å in the equilibrium geometry.

N1	(0, 0, 0.724500)
N2	(0, 0, −0.724500)
H3	(0.938543, 0.209092, 1.052800)
H4	(−0.209021, −0.938472, 1.052800)
H5	(−0.938543, 0.209092, −1.052800)
H6	(0.209021, −0.938472, −1.052800)

the normal coordinate approach gives prescriptions only for the displacement of the atomic sites of the molecule. To overcome this problem, we used the following simple model: When displacing atoms, the binding sites are constrained to remain on the implied bonds, sliding such as to conserve proportional distances from the atoms defining the bond. As regards the lone pair electrons, they remain located on the sum of the unit vectors of the three bonds formed by the nitrogen within a particular amino group, at a distance from the nitrogen atom varying proportionally to the modulus of the vector defining the resulting direction.

B. Systematic model potential

A new model potential has been developed to represent the intermolecular potential of the hydrazine dimer. The potential consists of a detailed atom-atom anisotropic representation of the multipolar electrostatic energy, dipole polarizabilities and dipole-dipole dispersion energy coefficients centered on the nitrogen atoms only, and simple atom-atom isotropic repulsion and penetration contributions:

$$E = E_{\text{mult}} + E_{\text{ind}} + E_{\text{disp}} + E_{\text{rep}} + E_{\text{pen}}. \tag{3}$$

Each of the components is described in more detail below. They are obtained mainly from *ab initio* monomer wave functions, using a modification of a systematic potential method described previously for chlorine-chlorine[21] and ion-water[23] interactions. There are considerable advantages inherent in using SCF monomer calculations rather than supermolecule calculations: Monomer calculations are free of basis set superposition error; only one or a few monomer calculations are required, whereas supermolecule calculations have to cover a six-dimensional intermolecular configuration space; supermolecule calculations give only an estimate of the total potential energy, which is difficult to correct for basis set and correlation effects, whereas monomer calculations give physically meaningful components such as those in Eq. (3). These components can be adjusted if necessary to reproduce known molecular properties such as multipoles and polarizabilities. It is also easier to find reasonable functional forms that fit the components in Eq. (3) separately, rather than fitting the total potential energy obtained from supermolecule calculations.

Monomer hydrazine wave functions were calculated in the SCF approximation using the CADPAC *ab initio* package,[24] with a CADPAC library 8s6p3d basis set on the nitrogen atoms, and 6s3p on the hydrogens. The geometry used corresponds to the experimental equilibrium structure, the atomic positions are shown in Table III. The SCF energy is $-111.23124\ E_h$.

The anisotropic features of the intermolecular potential are defined using molecule-fixed axes, which are oriented as follows: $\hat{\mathbf{z}}$ points from N2 to N1, $\hat{\mathbf{y}}'$ points from the center of mass of the four H atoms to the center of the two N atoms, $\hat{\mathbf{x}} = \hat{\mathbf{y}}' \times \hat{\mathbf{z}} / |\hat{\mathbf{y}}' \times \hat{\mathbf{z}}|$, and $\hat{\mathbf{y}} = \hat{\mathbf{z}} \times \hat{\mathbf{x}}$. The origin of molecular coordinates is the center of the two N atoms. This coordinate system is used in Table III. The direction of $\hat{\mathbf{x}}$ is reversed if necessary so that it makes an angle of less than 90° with the H5→H3 vector; the resulting left-handed set of axes would be required for the mirror image of the coordinates in Table III.

1. Multipolar electrostatic energy

The multipolar electrostatic energy is taken to be a sum of interactions between atomic multipoles that depend on the molecular geometry

$$E_{\text{mult}} = \sum_a \sum_b \sum_{lm} \sum_{l'm'} Q^a_{lm} Q^b_{l'm'} T_{lm,l'm'}(\Omega_{ab}) R_{ab}^{-(l+l'+1)}, \tag{4}$$

where R_{ab} is the distance between atom a on molecule A and atom b on molecule B, Q^a_{lm} and $Q^b_{l'm'}$ are atomic multipoles, and $T_{lm,l'm'}$ is an interaction tensor that depends on the direction of the vector $\mathbf{R}_{ab}$ relative to the molecule-fixed axes. The T tensors have been tabulated by Price *et al.*[25] In this work, the sum in Eq. (4) is truncated at $l + l' = 2$, so the electrostatic energy consists of charge-charge, charge-dipole, charge-quadrupole and dipole-dipole contributions. Since these contributions occur for each pair of atoms, this is a detailed representation of the electrostatic energy. A higher percentage accuracy is required for the electrostatic energy than for the other components of the potential, because in hydrogen-bonded dimers the electrostatic energy usually gives the largest contribution to both the magnitude and the anisotropy of the potential.

Atomic multipoles are calculated from the SCF wave functions by dividing the charge density into discrete atomic pieces, then calculating the multipoles of each piece in the coordinate system of its associated atom. The atomic coordinate system of each atom has axes parallel to the molecular axes, and an origin at the atomic nucleus. The distributed multipole analysis technique of Stone and Alderton[26] is used to partition the charge density; this method is known to give good convergence with increasing multipole rank. The resulting atomic multipoles are shown in Table IV.

TABLE IV. Atomic multipoles for hydrazine in its equilibrium structure, in atomic units.

N1	$Q_{00}=-0.273161$			
	$Q_{10}=-0.355724$	$Q_{11c}=0.242167$	$Q_{11s}=-0.185758$	
$Q_{20}=0.713929$	$Q_{21c}=0.118305$	$Q_{21s}=-0.404812$	$Q_{22c}=-0.078755$	$Q_{22s}=0.701852$
N2	$Q_{00}=-0.273161$			
	$Q_{10}=0.355724$	$Q_{11c}=-0.242167$	$Q_{11s}=-0.185758$	
$Q_{20}=0.713929$	$Q_{21c}=0.118305$	$Q_{21s}=0.404812$	$Q_{22c}=-0.078755$	$Q_{22s}=-0.701852$
H3	$Q_{00}=0.161953$			
	$Q_{10}=0.034588$	$Q_{11c}=0.120732$	$Q_{11s}=0.024491$	
$Q_{20}=0.016771$	$Q_{21c}=0.019403$	$Q_{21s}=-0.019585$	$Q_{22c}=0.014077$	$Q_{22s}=0.060056$
H4	$Q_{00}=0.111207$			
	$Q_{10}=0.032402$	$Q_{11c}=-0.048437$	$Q_{11s}=-0.119053$	
$Q_{20}=0.031568$	$Q_{21c}=0.021698$	$Q_{21s}=-0.015449$	$Q_{22c}=-0.043420$	$Q_{22s}=0.022251$
H5	$Q_{00}=0.161953$			
	$Q_{10}=-0.034588$	$Q_{11c}=-0.120732$	$Q_{11s}=0.024491$	
$Q_{20}=0.016771$	$Q_{21c}=0.019403$	$Q_{21s}=0.019585$	$Q_{22c}=0.014077$	$Q_{22s}=-0.060056$
H6	$Q_{00}=0.111207$			
	$Q_{10}=-0.032402$	$Q_{11c}=0.048437$	$Q_{11s}=-0.119053$	
$Q_{20}=0.031568$	$Q_{21c}=0.021698$	$Q_{21s}=0.015449$	$Q_{22c}=-0.043420$	$Q_{22s}=-0.022251$

2. Induction and dispersion energy

The induction energy of molecule A consists of one contribution from each nitrogen atom of A, as follows:

$$E^A_{\rm ind}=-\frac{1}{2}\sum_{a\in N}\alpha_{xx}(F^a_{11c})^2+\alpha_{yy}(F^a_{11s})^2+\alpha_{zz}(F^a_{10})^2 +2\alpha_{xz}F^a_{11c}F^a_{10}. \quad (5)$$

The electrostatic field components F^a_{lm} are produced by the atomic multipoles of all other molecules B

$$F^a_{lm}=-\sum_b\sum_{l'm'}Q^b_{l'm'}T_{lm,l'm'}(\Omega_{ab})R^{-(l+l'+1)}_{ab}, \quad (6)$$

and α_{xx}, α_{yy}, α_{zz}, α_{xz} are atomic polarizabilities, which are half the molecular polarizabilities. An analogous expression is used for the induction energy of the other molecules in the cluster. Higher-order effects, such as hyperpolarizabilities, quadrupole polarizabilities and interactions between induced multipoles are neglected, and the multipole rank l' in Eq. (6) is restricted to 0 and 1 (charges and dipoles). The dispersion energy consists of C_6 (dipole-dipole) contributions between each pair of nitrogen atoms

$$E_{\rm disp}=-\sum_{a\in N}\sum_{b\in N}\sum_{mm'}C_{lm,lm'}[T_{lm,lm'}(\Omega_{ab})]^2R^{-6}_{ab}, \quad (7)$$

where the atomic dispersion energy coefficients C are one-quarter of the molecular dispersion energy coefficients. Higher-rank dispersion energy coefficients are neglected.

CHF molecular polarizabilities and TDCHF dispersion energy coefficients were calculated using the CADPAC package, with the basis set described above. It is found that the dispersion energy coefficients obey to within 0.2% the relationship $C_{lm,l'm'}=c_{lm}c_{l'm'}$. ''Mixed'' dispersion energy coefficients are found to be negligible. The atomic polarizabilities and atomic c coefficients (half the molecular C coefficients) are given in Table V. The polarizabilities and dispersion energy coefficients are empirically scaled in the final model potential, in an attempt to correct for neglect of correlation. No literature values are available, so an analogous *ab initio* calculation using the same basis set was performed on NH_3, with N–H bondlengths of 1.017 Å, and HNH bond angles of 107.8°. This gave an isotropic polarizability of 12.53 a.u., and a spherical dispersion energy coefficient of 75.40 a.u. The accurate values are 14.56 and 89.08, respectively.[27] Making the assumption that the scaling required for hydrazine is the same as for ammonia, the atomic polarizabilities in Table V are multiplied by 1.16, and the c coefficients by 1.09.

3. Repulsion energy

Although the repulsion energy cannot be computed exactly from monomer wave functions, there are several empirical models[28,29] that relate it to monomer properties, usually with one or more fitted parameters. In this work, the overlap model[29] is used

$$E_{\rm rep}=KS^x_\rho, \quad (8)$$

where K and x are adjustable parameters, S_ρ is the electronic charge density overlap integral

$$S_\rho=\int\rho^A_{\rm el}(\mathbf{r})\rho^B_{\rm el}(\mathbf{r})d\mathbf{r}, \quad (9)$$

ρ^A_{el} and ρ^B_{el} are the electron densities of molecule A and B.

The charge density overlap integral was calculated for 200 relative orientations of the hydrazine dimer. The orientations were randomly chosen, with the restriction that the closest N–N intermolecular contact was between 4 and 6

TABLE V. Atomic polarizabilities and c coefficients for the nitrogen atoms of hydrazine, in atomic units. Dispersion coefficients are a product of two c coefficients, as shown in the text. Before using these values in the model potential, the polarizabilities should be multiplied by 1.16, and the c coefficients by 1.09.

$\alpha_{xx}=19.077$	$\alpha_{yy}=19.019$	$\alpha_{zz}=23.831$	$\alpha_{xz}=1.208$
$c_{11c}=5.5584$	$c_{11s}=5.5486$	$c_{10}=6.6411$	

a_0, and other atom-atom contacts were longer than 3.2 a_0. The GMUL program[30] was used to perform the integrations, using charge densities calculated from the SCF monomer wave functions. The resulting overlap integrals were fitted using a simple atom-atom exponential function,

$$S_\rho = \sum_{ab} A_{ab} \exp(-\alpha_{ab} R_{ab}). \tag{10}$$

The best-fit parameters, with all points included, are $A_{ab} = 22.42$ a.u., $\alpha_{ab} = 1.891\ a_0^{-1}$ for N–N; $A_{ab} = 2.86$ a.u., $\alpha_{ab} = 2.056\ a_0^{-1}$ for N–H. The rms percentage error is 14.2%. Including H–H contributions reduces the error by less than 0.1%. It has not been found necessary in this work to make A (or α) anisotropic, although this has been done in the past for other dimers,[21,31] and can give significant improvements in the potential.[31]

The parameters K and x in Eq. (8) still have to be obtained. It is assumed here that $x = 1$, in accordance with physical intuition and with the results of some earlier work. The scaling parameter K is discussed below.

4. Penetration energy

The multipolar electrostatic energy, given by Eq. (2), is part of the total first-order Coulomb interaction energy between two molecules:

$$E_C^{(1)} = \int\int \rho^A(\mathbf{r}_1)\rho^B(\mathbf{r}_2) r_{12}^{-1} d\mathbf{r}_1\, d\mathbf{r}_2, \tag{11}$$

where ρ^A and ρ^B are the electronic plus nuclear charge densities. For some dimers it is sufficient to use Eq. (4) as a reasonable approximation to Eq. (11). However, for hydrogen-bonded dimers, there is strong evidence that the difference between the multipolar and Coulomb energies, called the penetration energy, is quite large. Calculations suggest that it can contribute 20% or more to the binding energy. The current hydrazine potential therefore includes a specific penetration term.

The penetration energy $E_{\text{pen}} = E_C^{(1)} - E_{\text{mult}}$ has been calculated, using the GMUL program, at the 200 geometries used for the charge density overlap. It is fitted to an atom-atom isotropic form

$$E_{\text{pen}} = \sum_{ab} B_{ab} \exp(-\beta_{ab} R_{ab}) \tag{12}$$

giving $B_{ab} = -49.40$ a.u., $\beta_{ab} = 1.864\ a_0^{-1}$ for N–N, and $B_{ab} = -6.659$ a.u., $\beta_{ab} = 2.056\ a_0^{-1}$ for N–H. The rms percentage error is 16.0%. In agreement with previous calculations on different dimers, the penetration energy is found to be negative for physically accessible intermolecular geometries, whereas both $E_C^{(1)}$ and E_{mult} change sign with orientation.

III. STRUCTURE CALCULATIONS

Cluster structure calculations can be straightforwardly performed by minimizing the total interaction energy of the cluster components. Despite the very simple underlying idea, such calculations can be quite cumbersome even for not very large clusters (typically composed of more than five molecules) due to the rapid increase of the number of structural parameters with the cluster size.

Taking into account the different nature of the interaction forces and the different magnitudes of the corresponding binding energies for the intra- and intermolecular degrees of freedom, a reasonable approach is to consider the molecules ''frozen'' and to minimize the intermolecular potential with respect to the relative positions of the component molecules. Moreover, such a technique is fully consistent with the overall philosophy of the *frozen molecule approach* for calculating the frequency shifts.

The position and orientation of each molecule, kept rigid in its equilibrium configuration, is specified by the three Cartesian coordinates of its center of mass and by three Euler angles. In order to find local minima of the potential energy hypersurface, these intermolecular degrees of freedom are optimized without constraints starting from randomly chosen initial configurations, using the NAG library routine E04JAF, which is based on a Newton-like algorithm. Typically, several hundreds up to thousands of minimizations are necessary to yield the global minimum for a particular cluster size.

As a general remark, it is noteworthy that the only cluster size which yields for both potential models (EPEN/2 and the systematic potential) a defined number of stable configurations is the dimer, for which we obtained three energetically well separated minima. For the larger clusters well separated absolute minima result which are typically 1 kJ/mol apart from the rest of the minima. But then very close lying higher energy configurations are obtained tending to form with increasing cluster size a dense number of isomers.

In order to determine the parameter K of Eq. (8) we have calculated the lowest energy dimer configuration, the cyclic arrangement, for the three different parameters $K = 5$, 6, and 7. The resulting well depths are -32.01, -23.99, and -19.77 kJ/mol and the NH distances are 2.019, 2.228, and 2.374 Å, respectively. These values can be compared with the results of *ab initio* calculations. For the dimer of the same structure CEPA calculations give binding energies of -24.62 to -25.53 kJ/mol, depending somewhat on the basis set with an N-H distance of 2.22 Å.[32] The NH distance can also be compared with that of similar systems. For the well studied ammonia dimer the value 2.24 Å results,[33] while for the system NCH-NH_3 2.15 Å is obtained.[34] The value $K = 6$ reproduces all these results best, and it will be used in the further course of this work. This comparison also indicates that the lowest energy isomer of the EPEN/2-potential has with -18.69 kJ/mol a smaller well depth and with 2.538 Å a larger NH distance than the optimal value.

There are no experimental second virial coefficients for hydrazine available in the literature. Nevertheless we present here calculations of this property for the two potential models using the classical approximation. For the evaluation of the temperature dependence of the second virial coefficient of hydrazine we have employed Monte Carlo quadratures, achieving for 10^6 integration points a typical precision of

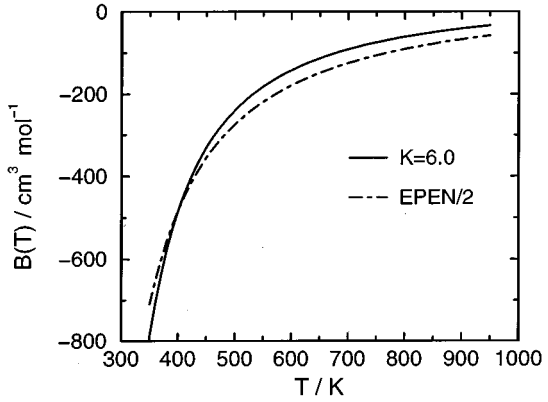

FIG. 1. Second virial coefficient of hydrazine as a function of temperature for the systematic and for the EPEN/2 potential.

3%. We have depicted in Fig. 1 the plots of the virial coefficients for the systematic potential and the EPEN/2 potential. It can be easily seen that the results of the two potentials are quite different, giving steeper curves for the systematic potential.

The results of our configuration calculations with the systematic potential are summarized in Table VI(a), where the binding energies and the mean hydrogen bond lengths for the three lowest lying isomers of each hydrazine cluster size, ranging from dimer to hexamer, are listed. The assignment of hydrogen bonds can be uniquely done for the dimer and trimer configurations, but it becomes ambiguous for larger clusters. Two somewhat contrary requirements determine the mean hydrogen bond lengths. First, for a given cluster size the energetically lower configurations maximize the number of hydrogen bonds, since these give the main contribution to the binding energy. Second, for isomers with the same number of hydrogen bonds the ones will be preferred which consist of geometrically relaxed bonds.

TABLE VI. (a) Binding energies (in kJ/mol) and mean hydrogen bond lengths (in Å) of the three lowest lying isomers for each cluster size, obtained by means of the systematic potential with repulsive potential parameter $k=6.0$. (b) Binding energies (in kJ/mol) and mean hydrogen bond lengths (in Å) of the three lowest lying isomers for each cluster size, obtained by means of the EPEN/2 potential.

M	$-E$	d	$-E'$	d'	$-E''$	d''
			(a)			
2	23.99	2.228	22.08	2.379	17.56	2.412
3	55.52	2.144	54.42	2.161	53.60	2.168
4	94.86	2.150	91.44	2.163	90.82	2.144
5	129.38	2.180	128.74	2.271	128.64	2.174
6	169.29	2.181	169.20	2.215	168.77	2.187
			(b)			
2	18.69	2.538	17.94	2.525	17.51	2.685
3	45.40	2.464	45.05	2.441	43.51	2.457
4	76.70	2.540	76.68	2.501	75.83	2.516
5	111.07	2.536	110.06	2.502	105.94	2.522
6	145.14	2.475	142.71	2.528	140.07	2.530

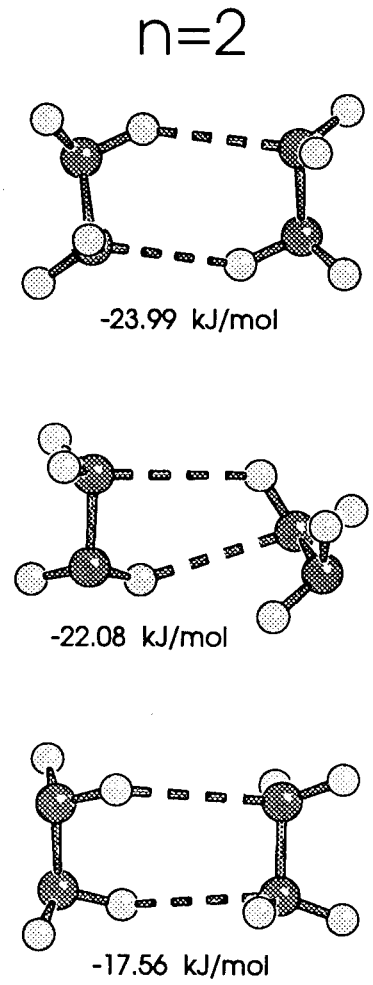

FIG. 2. The three energetically most stable hydrazine dimer structures for the systematic potential.

For the dimer and trimer, the mean hydrogen bond lengths decrease monotonically when going from the energetically higher configurations to the minimum. As can be seen in Figs. 2 and 3 the three lowest configurations for these clusters all prefer ring structures with two bonds for the dimer and three bonds for the trimer. In view of the sp^3-hybridization of the nitrogen atoms in the hydrazine molecule, it is obvious that the lowest energy dimer should have the most relaxed structure. The deviation of the sp^3-orbitals from their ideal tetrahedral structure is smallest, the lone pair electrons are far apart. In this configuration the N atom of one amino group and one H atom of the other amino group of the same hydrazine molecule act as acceptor and donor for the other molecule. In the second lowest energy configuration the situation is similar, aside from the fact that in one molecule only one amino group is involved acting as donor and acceptor at the same time. In the third lowest energy configuration one molecule consists of two donor and the other of two acceptor atoms. Note that the lowest and third lowest dimer configurations both have C_2-symmetry. In the latter one, however, the tension in the bonds is much higher, as the increase in the mean bond lengths indicates. The position of the lone pair electrons is less optimal.

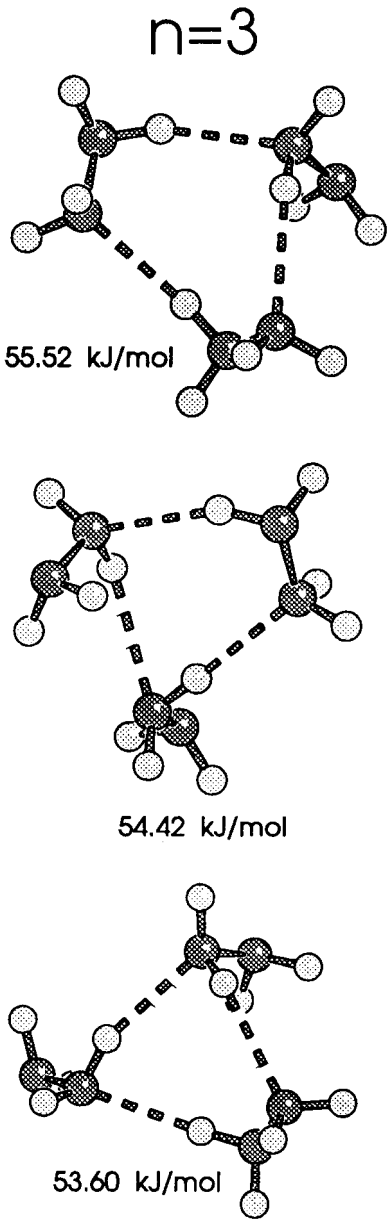

FIG. 3. The three energetically most stable hydrazine trimer stuctures for the systematic potential.

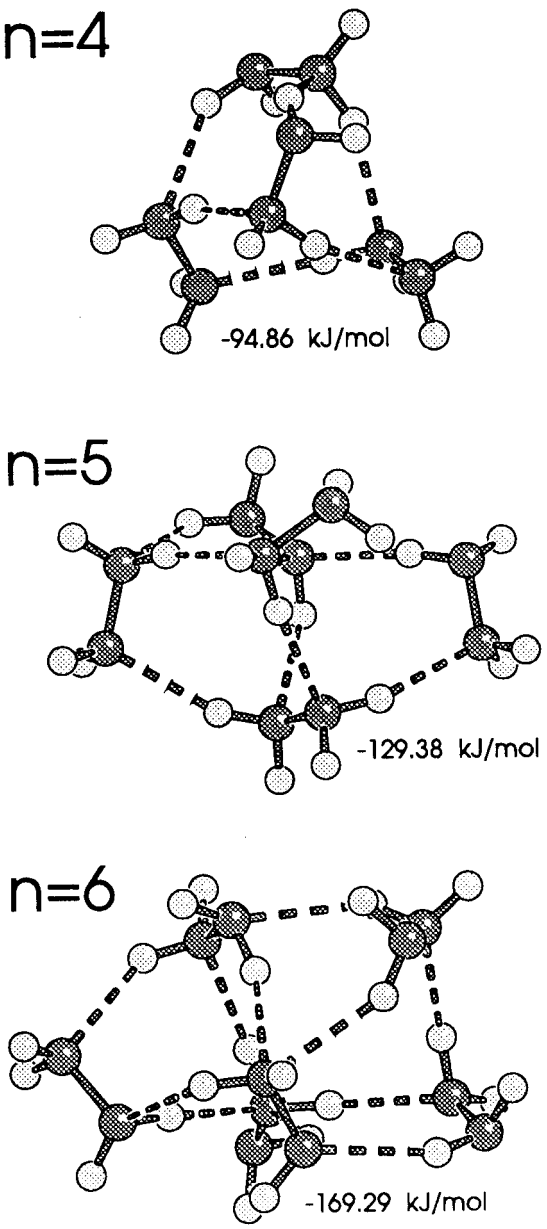

FIG. 4. The energetically most stable hydrazine tetramer, pentamer, and hexamer stuctures for the systematic potential.

For the lowest energy trimer it is noticed that for two molecules the donor and acceptor amino groups are different, while for the other two configurations this is the case only for one molecule. A decrease in the mean hydrogen bond lengths is expected for ring structures of increasing size because of the cooperativity effect. This is clearly observed for the lowest energy dimer and trimer configurations. From the tetramer onwards, however, no systematic behavior results, an indication of a structural change. In Fig. 4 the lowest energy tetramer, pentamer, and hexamer structures are shown. They all exhibit three-dimensional structures.

For the tetramer a combination of the lowest energy trimer with one molecule on top of it can be recognized. The number of hydrogen bonds is increased tremendously from three for the trimer to six for the tetramer. The bonds are not as optimal as in the trimer which yields a slightly increased mean hydrogen bond length. The lowest energy configuration for the pentamer is again quite symmetric. The change from two-dimensional structures to three-dimensional structures can also be seen in the plot of the incremental binding energy $E_n - E_{n-1}$ as a function of the cluster size n in Fig. 5. A pronounced maximum is found for $n=4$. Comparing the plots for the lowest and second lowest energy configurations the main difference is found for the tetramer and pentamer.

In Table VI(b) we have given the results of our configuration calculations for the EPEN/2 potential. It is noted by comparing them with the corresponding results of the systematic potential that the binding energies are typically 15%–20% smaller with respect to the systematic potential. The plot of the incremental binding energy for the lowest

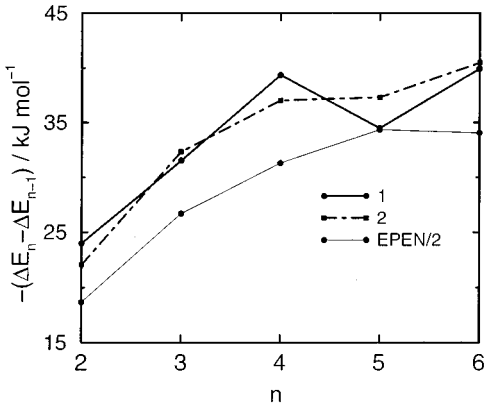

FIG. 5. Incremental binding energies of small hydrazine clusters versus cluster size for the systematic and the EPEN/2 potential. 1 and 2 designate the plot for the lowest and the second lowest energy cluster configurations for the systematic potential, respectively.

energy configurations in Fig. 5 shows a similar profile as the one found for the second lowest isomers of the systematic potential.

Figure 6 presents the most stable hydrazine cluster structures from trimer up to the pentamer for the EPEN/2 potential. The dimers have the same shape and symmetry properties as those obtained for the systematic potential. It is, however, noteworthy that, apart from having different binding energies and hydrogen bond lengths, the energetical order of the EPEN/2 configurations is different: Going from the lowest energy structure to the third lowest one, the corresponding figures should be considered in the sequence 3c, 3a, and 3b. This sequence is somewhat surprising in view of the results obtained for the systematic potential. The remaining EPEN/2 clusters have different shapes as compared to the ones determined by the systematic potential. Two features, however, are very similar: First, with both potentials ring structures are found for the lowest energy dimer and trimer. Second, for the tetramer and larger clusters three-dimensional structures are found. Aside from the dimer, symmetric structures are usually not obtained for the lowest energy configurations.

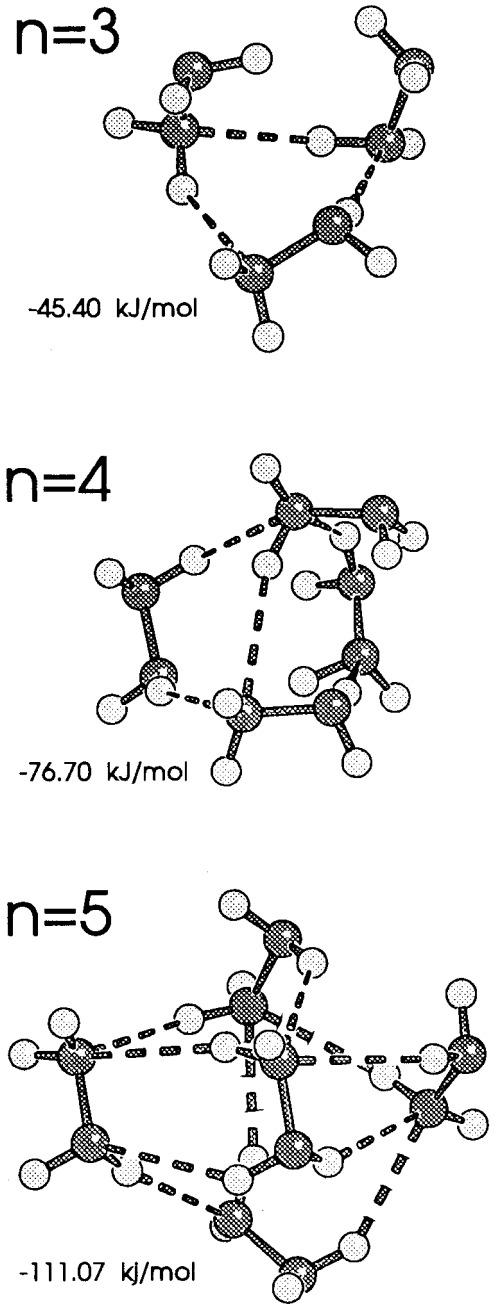

FIG. 6. The lowest energy hydrazine trimer, tetramer, and pentamer structures for the EPEN/2 potential.

IV. THE FROZEN MOLECULE APPROACH

The total cluster Hamiltonian may be written within the FMA as

$$H=\frac{hc}{2}\sum_{r=1}^{3N-6}\sum_{m=1}^{M}\omega_r(p_{rm}^2+q_{rm}^2)+\frac{hc}{6}\sum_{r,s,t=1}^{3N-6}\sum_{m=1}^{M}\phi_{rst}q_{rm}q_{sm}q_{tm}+U, \tag{13}$$

where the first sum describes the uncoupled harmonic oscillations, the second sum is the anharmonic correction, while U represents the intermolecular potential. Here, ω_r and ϕ_{rst} are the harmonic frequencies and the cubic force constants in units of wave numbers, respectively. q_{rm} and p_{rm} are position and momentum operators associated with normal mode r of molecule m. M stands for the number of identical N-atomic molecules. The first two sums of the Hamiltonian (13) describe the conventional normal mode approach for the individual molecules including cubic anharmonicities.

In view of the fact that the Hamiltonian (13) is dominated by the harmonic term (first sum), which in addition allows for a full analytical diagonalization, the anharmonic term and the intermolecular potential can be treated as a perturbation

$$W=\frac{hc}{6}\sum_{r,s,t=1}^{3N-6}\sum_{m=1}^{M}\phi_{rst}q_{rm}q_{sm}q_{tm}+U. \tag{14}$$

The first order correction to the non-degenerate ground state energy is readily obtained as the mean value of the perturbation in the ground state

$$\varepsilon_0^{(1)}=\langle 0|W|0\rangle=U_0+\frac{1}{4}\sum_r\sum_m\frac{\partial^2 U}{\partial q_{rm}^2}, \tag{15}$$

where U_0 is the interaction energy of the molecules frozen in their equilibrium position. The first order energy corrections $\varepsilon_{ni}^{(1)}$ (with n the eigenstate index and i the degeneracy index) result as eigenvalues of the perturbation matrix in the representation defined by the basis vectors $|1_{ni}\rangle$ which span the subspace of the respective energy level

$$\sum_{j=1}^{M}[\langle 1_{ni}|W|1_{nj}\rangle-\varepsilon_{ni}^{(1)}\delta_{ij}]c_{ji}^n=0,\quad i=1,2,\ldots,M. \tag{16}$$

Here are the expressions for the perturbation matrix elements

$$\langle 1_{ni}|W|1_{ni}\rangle=U_0+\frac{1}{4}\sum_r\sum_m\frac{\partial^2 U}{\partial q_{rm}^2}+\frac{1}{2}\frac{\partial^2 U}{\partial q_{ni}^2}, \tag{17}$$

$$\langle 1_{ni}|W|1_{nj}\rangle=\frac{1}{2}\frac{\partial^2 U}{\partial q_{ni}\partial q_{nj}},\quad i\neq j. \tag{18}$$

Diagonalization of the perturbation matrix yields besides the first order energy corrections $\varepsilon_{ni}^{(1)}$, the coefficients c_{ji}^n. As is apparent from Eqs. (15) and (18), neither the first order ground state energy correction nor the corrections of the simply excited states imply cubic force constants, that is, the first order line shifts are independent of the intramolecular force constants, depending only on the intermolecular potential.

The first order line shift can thus be expressed as

$$\Delta\nu_{ni}^{(1)}=\frac{\varepsilon_{ni}^{(1)}-\varepsilon_0^{(1)}}{hc}, \tag{19}$$

with $\varepsilon_{ni}^{(1)}$ determined numerically from the eigenvalue Eq. (16) of the perturbation matrix and $\varepsilon_0^{(1)}$ given by Eq. (15).

As for the second order line shift, $\varepsilon_{njk}^{(2)}$, the FMA yields the expression:

$$\Delta\nu_{ni}^{(2)}=\frac{1}{\Sigma_j|c_{ji}^n|^2}\sum_{j,k}c_{ji}^n c_{ki}^{n*}\Delta\nu_{njk}^{(2)}, \tag{20}$$

where

$$\begin{aligned}\Delta\nu_{njk}^{(2)}=&-\frac{\delta_{jk}}{2}\sum_r\frac{3-\delta_{rn}}{2}\frac{\phi_{nnr}}{\omega_r}\left(\frac{\partial U}{\partial q_{rj}}\right)\\&-\frac{1}{4(hc)^2}\sum_r\sum_m\left[\frac{1}{\omega_n+\omega_r}\right.\\&\left.-\frac{1-\delta_{rn}}{\omega_n-\omega_r}\right]\frac{\partial^2 U}{\partial q_{nj}\partial q_{rm}}\frac{\partial^2 U}{\partial q_{nk}\partial q_{rm}}.\end{aligned} \tag{21}$$

Generally, the most significant contributions to the second order line shifts are due to the first sum of this expression, containing the generalized forces $-\partial U/\partial q_{rj}$ and the intramolecular force constants ϕ_{nnr}. The second sum of Eq. (21) is essentially less important due to the presence of the second order derivatives of the intermolecular potential and describes the coupling of the normal modes of the individual molecules by the potential solely. However, through the resonance terms contained in the second sum, close lying levels can sometimes substantially contribute to the frequency shift.

The total frequency shift of a particular cluster spectral band finally results as the sum of the corresponding first and second order shifts

$$\Delta\nu_{ni}=\Delta\nu_{ni}^{(1)}+\Delta\nu_{ni}^{(2)}. \tag{22}$$

The details of the necessary calculations of the derivatives of the potential are given in Appendix B of Ref. 12.

The relative importance of the cluster spectral line corresponding to a particular normal mode can be judged on the basis of the infrared intensity calculated from the square of the transition dipole moment.[11,12]

We note that the truncation of the Hamiltonian Eq. (13) after the cubic term is sufficient as long as only relative frequency shifts are calculated.[35] The inclusion of the quartic term in first order perturbation theory changes the intramolecular energy levels and frequencies because of the additional anharmonicity in the intramolecular potential, but in the final result for the term differences this part cancels and the terms of Eqs. (19) and (20) are left in which the second term contains only cubic force constants coupled to the first derivatives of the intermolecular potential.

V. FREQUENCY SHIFTS

As was already pointed out, the second order frequency shifts given by Eqs. (20) and (21) depend on the molecular cubic force constants ϕ_{nnr}, which describe the coupling of the considered mode to the other intramolecular modes. Usually, from *ab initio* calculations force constants result in the representation of the curvilinear internal valence coordinates. In order to be used in the perturbation approach described in the preceding section, the force constants must undergo a transformation from internal- to normal coordinates. This transformation is accomplished as part of the normal mode analysis of the molecular vibrations, which also yields the anharmonic frequencies of the normal modes of the monomer.

All relevant data needed for the normal mode analysis of the hydrazine molecule (internal coordinates and force constants) are taken from Ref. 19, where the force field of the hydrazine has been evaluated from *ab initio* SCF calculations with a standard 4-31G basis set. The hydrazine monomer may be conveniently described using 12 unsymmetrized internal coordinates grouped in two symmetry species. Harmonic force constants are provided for all internal coordinates, and, in order to account for anharmonicity, all cubic

TABLE VII. Lineshifts $\Delta\nu_5$ ($\nu_5=1098$ cm^{-1}, NN stretch) and $\Delta\nu_{12}$ ($\nu_{12}=937$ cm^{-1}, NH_2 wag) of the experiment[18] the EPEN/2 potential, and the systematic potential.

	ν_5					ν_{12}				
	Expt.	EPEN/2		Syst. pot.		Expt.	EPEN/2		Syst. pot.	
M	$\Delta\nu$	$\Delta\nu$	I_{rel}	$\Delta\nu$	I_{rel}	$\Delta\nu$	$\Delta\nu$	I_{rel}	$\Delta\nu$	I_{rel}
2	−16	−10.0	0.05	0.93	0.02	42	−35.5	0.03	32.29	0.33
		0.9	0.22	3.22	0.06	48	−19.2	0.78	61.43	0.12
3	−10	−12.6	0.13	4.43	0.06	55	−38.9	0.63	56.01	0.28
		−8.7	0.04	4.89	0.06		−31.0	0.64	59.56	0.14
		−0.1	0.23	8.28	0.02	88	−6.4	0.05	87.75	0.25
4		−12.2	0.06	4.00	0.02		−50.0	0.07	64.97	0.15
		−8.9	0.15	6.41	0.04		−39.8	0.24	70.41	0.14
		−6.6	0.13	8.81	0.02	88	−39.2	0.42	85.60	0.29
		−3.1	0.12	10.62	0.09	109	−38.8	0.96	106.78	0.32
5		−15.6	0.02	5.70	0.07		−50.7	0.51	65.33	0.08
		−9.8	0.10	6.28	0.03		−50.6	0.65	72.57	0.23
		−6.9	0.07	8.84	0.05	88	−41.1	0.13	88.68	0.45
		−5.1	0.13	10.92	0.02		−34.4	0.21	88.92	0.35
		−1.3	0.25	20.16	0.04	112	−24.3	0.61	102.19	0.02
6		−17.5	0.02	6.88	0.05		−72.0	0.98	80.20	0.08
		−17.2	0.09	7.79	0.02		−62.7	0.34	82.87	0.13
		−6.1	0.03	8.06	0.02	89	−36.7	0.13	93.59	0.30
		−2.9	0.34	10.16	0.06		−35.5	0.28	101.31	0.09
		0.3	0.18	12.01	0.07		−22.2	0.54	113.56	0.06
		9.4	0.12	21.84	0.04	112	−18.7	0.37	118.68	0.68

force constants of the form F_{ij} and quartic force constants of the form F_{iiii} for the bond stretching coordinates are included.

Using the force field of Ref. 19 we have computed the monomer harmonic frequencies by the Wilson *F-G* method.[36] The transformation of the force constants from internal to normal coordinates is carried out by employing the *L*-tensor approach of Hoy, Mills and Strey.[37] Special attention has been devoted to the treatment of the torsion coordinates, for which we have derived new compact analytical *L*-tensor formulas, described in detail elsewhere.[38]

In our line shift calculations, we have dealt only with two of the 12 normal modes of hydrazine: the NN stretching mode ($\nu_5=1098$ cm^{-1}), and the NH_2 wagging mode ($\nu_{12}=937$ cm^{-1}). The frequency shifts computed by means of the approach described above refer to these monomer lines.

VI. RESULTS

Now we are ready to compare the results of the calculations for the line shifts of the energetically lowest configurations using the two potential models introduced in the previous sections. They are given in Table VII together with the experimental observations. For the EPEN/2 potential the excitation of the N-N stretching mode (ν_5) gives small negative values up to -10 cm^{-1} for the dimer and shows only a small dependency on cluster size. In the case of the asymmetric NH_2-wagging mode (ν_{12}) the shifts are all negative in the range from -19 to -35 cm^{-1} for the dimer. The shifts increase up to -70 cm^{-1} with increasing cluster size. While the former results are in good agreement with experimental results which exhibit shifts between -16 and -8 cm^{-1}, the latter results are completely wrong, since the experimental values vary between 42 and 112 cm^{-1}. We note that the heavy particle motion of the N-N stretching mode which causes only small line shifts is reasonably well reproduced by this potential. The large amplitude motion of the light hydrogen atoms in the asymmetric NH_2-wagging mode, however, is not at all reproduced.

The results for the systematic potential are also given in Table VII. Now the N-N stretching mode shows small shifts of 1 to 10 cm^{-1} independent of the cluster size. This is in qualitative agreement with the experiments, although the sign is not correct. But the asymmetric NH_2-wagging mode exhibits indeed the large blueshifts ranging from 32 to 119 cm^{-1} that are observed in the experiments. For the trimer, the tetramer and the hexamer the results are within a few wave numbers in surprisingly good agreement with the measurements, if the shifts with the largest intensities are used. For the dimer and the pentamer some differences are observed. Since the measurements are partly incomplete because of some missing laser lines, we have conducted additional measurements and will present the results together with a more complete analysis which also includes the different isomers in the following paper which will hopefully clarify these points.

Since in both cases the frozen molecule approach was used to calculate the line shifts, the discrepancy in the results is obviously caused by the potential models. The good agreement with experimental results for the systematic potential

TABLE VIII. $\Delta\nu_{12}$ (ν_{12}=937 cm^{-1}) for the components of the systematic potential for the lowest energy dimer.

Tot.	Rep.	Mult.	Pen.	Ind.	Disp.
32.29	−18.01	38.88	6.32	2.85	0.72
61.43	−27.30	73.72	10.19	3.56	0.56

shows that the chosen methodological ansatz is even competitive for modes with large amplitude motion of the H atoms.

In order to get more insight into the problem of the origin of the line shifts, the contributions of the different terms in the systematic potential model to the overall line shift have been analyzed. The results for the most stable dimer are given in Table VIII. The long ranged attractive dispersion energy and induction terms play only a marginal role. The main contribution comes from the large blueshift of the electrostatic term (combining multipole and penetration contributions) which is reduced by the repulsive overlap term. This remains true for the larger cluster sizes up to the hexamer. It is just this electrostatic term which is very carefully modelled in the systematic potential ansatz. In the case of the EPEN/2 model, the simple prescription for the choice of charges along with constraints for the positions of these charges fails to reproduce the required accuracy. Therefore we conclude that at least for systems like hydrazine which are dominated by hydrogen bonds, the accurate calculation of the electrostatic term in the intermolecular potential is of crucial importance for the interpretation of the spectroscopic data.

ACKNOWLEDGMENTS

We thank Dr. V. Dyczmons and Professor P. Botschwina for the *ab initio* calculation of the hydrazine dimer and for sharing the results with us prior to publication. This work was supported by the Deutsche Forschungsgemeinschaft in the Schwerpunktprogramm ''Molekulare Cluster'' and the European Community by Contract SC1-CT91-0699.

[1] U. Buck, in *The Chemical Physics of Atomic and Molecular Clusters*, edited by G. Scoles (Oxford University Press, New York, 1988), p. 543.
[2] U. Buck, in *Clusters of Atoms and Molecules*, edited by H. Haberland (Springer, Heidelberg, 1994).
[3] D. J. Nesbitt, Chem. Rev. **88**, 843 (1988).
[4] J. R. Heath, R. A. Sheekes, A. L. Crosky, and R. J. Saykally, Science **249**, 855 (1990).
[5] T. E. Gough, R. E. Miller, and G. Scoles, J. Chem. Phys. **69**, 1588 (1978).
[6] R. E. Miller, Science **240**, 447 (1988).
[7] U. Buck, J. Phys. Chem. **92**, 1023 (1988).
[8] U. Buck and H. Meyer, J. Chem. Phys. **84**, 4854 (1986).
[9] U. Buck, J. Phys. Chem. **98**, 5190 (1994).
[10] U. Buck and B. Schmidt, J. Chem. Phys. **98**, 9410 (1993).
[11] T. A. Beu, Z. Phys. D **31**, 95 (1994).
[12] T. A. Beu and K. Takeuchi, J. Chem. Phys. **103**, 6394 (1995).
[13] U. Buck, X. J. Gu, C. Lauenstein, and A. Rudolph, J. Chem. Phys. **92**, 6017 (1990).
[14] U. Buck and M. Hobein, Z. Phys. D **28**, 331 (1993).
[15] F. Huisken and M. Stemmler, Chem. Phys. Lett. **144**, 391 (1988).
[16] F. Huisken and M. Stemmler, Z. Phys. D **24**, 277 (1992).
[17] F. Huisken, A. Kulcke, C. Laush, and J. M. Lisy, J. Chem. Phys. **95**, 3924 (1991).
[18] U. Buck, X. J. Gu, M. Hobein, C. Lauenstein, Chem. Phys. Lett. **163**, 455 (1989).
[19] N. Tanaka, Y. Hamada, Y. Sugawara, M. Tsuboi, S. Kato, and K. Morokuma, J. Mol. Spectrosc. **99**, 245 (1983).
[20] J. Snir, R. A. Nemenoff, and H. A. Scheraga, J. Phys. Chem. **82**, 2497, 2504 (1978).
[21] R. J. Wheatley and S. L. Price, Mol. Phys. **71**, 1381 (1990).
[22] M. Tsuboi and J. Overend, J. Mol. Spectrosc. **52**, 256 (1974).
[23] R. J. Wheatley and J. M. Hutson, Mol. Phys. **84**, 879 (1995); R. J. Wheatley, *ibid.* **87**, 1083 (1996).
[24] R. D. Amos, I. L. Alberts, J. S. Andrews, S. M. Colwell, N. C. Handy, D. Jayatilaka, P. J. Knowles, R. Kobayashi, N. Koga, K. E. Laidig, P. E. Maslen, C. W. Murray, J. E. Rice, J. Sanz, E. D. Simandiras, A. J. Stone, and M.-D. Su, CADPAC5: The Cambridge analytic derivatives package, Issue 5, Cambridge University Press, Cambridge, 1992.
[25] S. L. Price, A. J. Stone, and M. Alderton, Mol. Phys. **52**, 987 (1984).
[26] A. J. Stone, Chem. Phys. Lett. **83**, 233 (1981); A. J. Stone and M. Alderton, Mol. Phys. **56**, 1047 (1985).
[27] G. D. Zeiss and W. J. Meath, Mol. Phys. **33**, 1155 (1977).
[28] K. C. Ng, W. J. Meath, and A. R. Allnatt, Chem. Phys. **32**, 175 (1978); K. C. Ng, W. J. Meath, and A. R. Allnatt, Mol. Phys. **37**, 237 (1979); W. J. Meath and M. Koulis, J. Mol. Struct. (Theochem) **226**, 1 (1991), and references therein; R. J. Wheatley and W. J. Meath, Mol. Phys. **79**, 253 (1993).
[29] R. J. Wheatley and S. L. Price, Mol. Phys. **69**, 507 (1990).
[30] R. J. Wheatley and J. B. O. Mitchell, J. Comput. Chem. **15**, 1187 (1994); R. J. Wheatley, Mol. Phys. **79**, 597 (1993).
[31] P. M. Rodger, A. J. Stone, and D. J. Tildesley, Mol. Phys. **63**, 173 (1988); S. L. Price, *ibid.* **58**, 651 (1986); A. J. Stone and S. L. Price, J. Phys. Chem. **92**, 3325 (1988), and references therein.
[32] V. Dyczmons and P. Botschwina (unpublished).
[33] A. van der Avoird, E. H. T. Olthof, and P. E. S. Wormer, Faraday Discuss. Chem. Soc. **97**, 43 (1994).
[34] P. L. Moore Plummer and S. Chattopadhyay, Z. Phys. D **26**, 329 (1993).
[35] A. D. Buckingham, Proc. R. Soc. A **248**, 169 (1958).
[36] E. B. Wilson, J. C. Decius, and P. C. Cross, *Molecular Vibrations* (McGraw-Hill, New York, 1955).
[37] A. R. Hoy, I. M. Mills, and G. Strey, Mol. Phys. **24**, 1265 (1972).
[38] T. A. Beu, Z. Phys. D **26**, 263 (1993).